SAND2018-10936J

Phase modulation failsafe system for multi-kJ lasers based on optical heterodyne detection

D. J. Armstrong,[1] Q. M. Looker,[1] J. W. Stahoviak,[1] I. C. Smith,[1] J. E. Shores,[1] P. K. Rambo,[1] J. Schwarz,[1] C. S. Speas,[1] and J. L. Porter[1, a)]

Sandia National Laboratories, P.O. Box 5800, Albuquerque, New Mexico, 87185, USA

(Dated: 19 September 2018)

Amplification of the transverse scattered component of stimulated Brillouin scattering (SBS) can contribute to optical damage in the large aperture optics of multi-kJ lasers. Because increased laser bandwidth from optical phase modulation (PM) can suppress SBS, high energy laser amplifiers are injected with PM light. Phase modulation distributes the single-frequency spectrum of a master oscillator laser among individual PM sidebands, so a sufficiently high modulation index β can maintain the fluence for all spectral components below the SBS threshold. To avoid injection of single frequency light in the event of a PM failure, a high-speed PM failsafe system (PMFS) must be employed. Because PM is easily converted to AM, essentially all PM failsafes detect AM, with the one described here employing a novel configuration where optical heterodyne detection converts PM to AM, followed by passive AM power detection. Although the PMFS is currently configured for continuous monitoring, it can also detect PM for pulse durations ≥ 2 ns, and could be modified to accommodate shorter pulses. This PMFS was deployed on the Z-Beamlet Laser (ZBL) at Sandia National Laboratories, as required by an energy upgrade to support programs at Sandia's Z Facility such as magnetized liner inertial fusion (MagLIF). Depending on the origin of a PM failure, the PMFS responds in as little as 7 ns. In the event of an instantaneous failure during initiation of a laser shot, this response time translates to a 30–50 ns margin of safety by blocking a pulse from leaving ZBL's regenerative amplifier, which prevents injection of single frequency light into the main amplification chain. The performance of the PMFS, without the need for operator interaction, conforms to the principles of engineered safety.

a)Author to whom correspondence should be addressed: darmstr@sandia.gov

I. INTRODUCTION

Stimulated Brillouin scattering was first observed in quartz and sapphire in 1964,[1] and observation of transverse stimulated emission in liquids followed not long after in 1968.[2] Dampening effects measured in the 1970s suggested potentially large energy losses from SBS[3], and in the late 1980s damage to large optics in the Nova laser at Lawrence Livermore National Laboratory (LLNL) was attributed to SBS. Subsequent studies established conditions for initiation of transverse SBS described in terms of laser fluence (J/cm^2) and growth time, and demonstrated good agreement with analytical predictions of its threshold.[4–6] Subsequent use of optical phase modulation for line broadening demonstrated suppression of SBS in large windows used on Nova.[5] Additional studies of component failures on the Nova and Beamlet lasers at LLNL resulted in the design of failsafe lenses used as vacuum barriers.[7] Although redesigned optics enhance operational safety, all high energy laser systems now use PM line broadening for SBS suppression, and all require a PM failsafe system (PMFS). SBS can be suppressed using sinusoidal and non-sinusoidal phase modulation,[8–11] and it's also required for beam quality enhancement techniques such as smoothing by spectral dispersion (SSD).[12,13] Because PM is converted to AM by dispersion, gain narrowing, and étalon effects, and amplitude modulation alone enhances the risk of optical damage, all kJ-class lasers also employ methods to reduce AM generation during propagation through various stages of amplification.[14–18]

For many optical materials SBS can be suppressed using a single modulation frequency $f_\mathrm{m} \gtrsim 3$ GHz, and a sufficiently large modulation index, say $\gtrsim 5$, where the instantaneous phase of a sine modulated wave is given by $\phi(t) = 2\pi f_\mathrm{c} + \beta \sin(2\pi f_\mathrm{m} t)$, where f_c is the carrier frequency and $\beta = \Delta f / f_\mathrm{m}$ is the modulation index. Although use of a single f_m and β is sufficient to suppress SBS, in practice modulation schemes can be much more complex, and typically require multiple, higher modulation frequencies and perhaps larger βs. For example, direct-drive inertial confinement fusion (ICF) typically employs a multi-pulse temporal format with small pre-pulse "pickets," where each requires its own modulation frequency to reduce imprinting of plasma surface modulations. A main pulse follows the pickets, where two-dimensional SSD can require a different modulation frequency for dispersion in two orthogonal spatial directions. A laser front-end with this level of complexity is described in Ref.[10], and references therein.

The PM failsafe system described here is installed on the Z-Beamlet Laser (ZBL) at Sandia National Laboratories,[19] and employs a novel configuration where optical heterodyne detection converts to PM to AM, followed by passive detection of the AM power. Compared to kJ class lasers configured for applications such as direct-drive ICF, ZBL has a relatively simple front end that typically generates a single pre-pulse and a main pulse and it doesn't currently employ SSD, so its modulation requirements are also comparatively simple. ZBL's PMFS was designed to accommodate a single modulation frequency, with $f_{\rm m}$ and β currently set at 17.6 GHz and 5.52, respectively, a combination similar to those used previously for 1D SSD on the National Ignition Facility at LLNL.[10] Although $f_{\rm m} = 17.6$ GHz exceeds the nominal 3 GHz sufficient to suppress SBS, this choice of $f_{\rm m}$ could accommodate future needs of programs at Sandia's Z Accelerator such as MagLIF,[20] which might require 1D SSD to reduce laser-plasma instabilities and enhance coupling of laser pre-heat energy into magneto-inertial fusion targets.[21] Although $f_{\rm m}$ is currently set to a relatively high frequency, ZBL's heterodyne based PMFS would easily accommodate $f_{\rm m} = 3$ GHz, however for much lower frequencies, say $f_{\rm m} \lesssim 20$ MHz, the corresponding reduction in beat note frequency might require replacing the passive AM detection scheme described in Sec. III A with active demodulation. In addition, a lower beat note frequency should eventually increase the response time of the PMFS, however performance characteristics at lower frequencies were not measured.

Finally, the design and functionality of this PMFS conforms to Sandia's program of work planning and control by incorporating the principles of engineered safety. Unlike administrative controls, which rely on training, compliance, and operator attentiveness, engineered safety accommodates situations where attention and operator intervention may be inadequate. For example, although a PM failure at the last moment is unlikely, it's not impossible, and the fast response required to recognize events on ns time scales can be accomplished only by a PMFS based on a high bandwidth design. Similarly, the margin of safety described in Sec. IV G eliminates the possibility of full amplification of single frequency light by stopping a pulse as it leaves ZBL's regenerative amplifier, even though the margin is ≤ 50 ns. Although this level of engineered control could appear unwarranted, it's preferable to the alternative of expensive damage followed by extended downtime.

II. METHODS FOR HIGH-SPEED DETECTION OF OPTICAL PHASE MODULATION

A PMFS for kJ lasers should respond to small changes in the optical PM spectrum on ns time scales, even though the possibility of a PM failure requiring such fast response is expected to be low. In addition, any PMFS should achieve long-term reliability with a high degree of reproducibility in its ability to detect PM. For most high bandwidth applications, detection of PM light requires conversion to AM light, followed by optical detection and some form of electronic demodulation. Usually the frequency of the local oscillator (LO) is equal to the modulation frequency, $f_{\mathrm{LO}} = f_{\mathrm{m}}$, although demodulating to DC with an intermediate frequency $f_{\mathrm{IF}} = 0$, is not a requirement. Various mechanisms can perturb the PM spectrum to generate AM, such as material dispersion, spectral filtering, reflection or transmission in a fiber Bragg grating, or some variation or combination of these techniques. Heterodyne detection, which uses interference with a local oscillator wave, can also be used for AM generation.

Another consideration for the design of a PMFS involves detecting PM continuously, or discretely in time, for example from a train of pulses. Essentially all kJ lasers begin with a low-power CW master oscillator – typically a fiber laser with a narrow line width and long-term frequency and power stability – followed by pulse shaping using a high-bandwidth amplitude modulator driven by an arbitrary waveform generator (AWG). If PM at a single modulation frequency and single β can be applied prior to pulse formation, as is currently done for ZBL, its presence can be monitored continuously, and also autonomously with respect to timing signals that control the laser system. When PM is applied following pulse formation, be it single- or multi-PM frequencies and perhaps multiple βs, continuous, uninterrupted monitoring isn't possible. Consequently, the detection scheme will be dictated by the laser's front-end architecture, which for ICF drive may require applying different PM frequencies sequentially to the picket pulses, followed by application of additional PM frequencies to the main pulse. Although PM detection may be carried out for the main pulse alone, these complex pulse formats and multiple PM frequencies could require additional considerations for the design of a PMFS. Given ZBL's simple front end, where a single modulation frequency is applied prior to pulse formation, we selected continuous monitoring based on optical heterodyne detection. The DC signal that serves as the trigger for a PM

failure event is obtained by passive detection of the power in the heterodyne beat note.

III. HETERODYNE DETECTION OF PM: GENERATING THE BEAT NOTE FROM A SINGLE LASER SOURCE

The concept for optical heterodyne detection of PM is illustrated in Fig. 1. The essential characteristic of this approach is interference of two first-order PM sidebands. One sideband belongs to the main PM spectrum that's injected into ZBL, which has $\beta_{\text{main}} = 5.52$ and $f_{\text{m}} = 17.6$ GHz. The other sideband belongs to a reference PM spectrum with $\beta_{\text{ref}} \approx 2.41$ and $f_{\text{m}} = 14.0$ GHz, which serves as the LO to generate the heterodyne beat note at a frequency of 3.6 GHz. As shown in Fig. 2, locking an étalon to that sideband selects it alone from the reference PM spectrum and transmits it for mixing with the main PM spectrum in the 50/50 combiner.

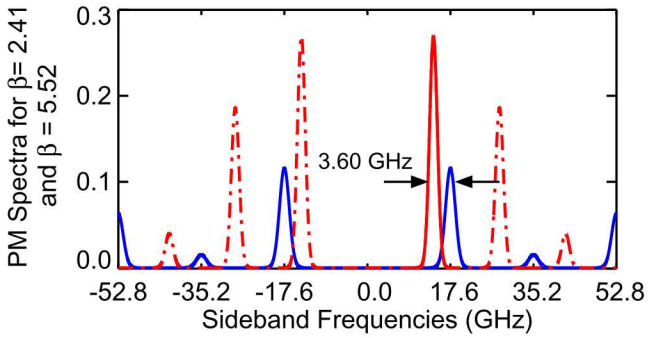

FIG. 1. Heterodyne detection of PM. First-order sideband interference for PM spectra with $\beta_{\text{main}} = 5.52$ and $f_{\text{m}} = 17.6$ GHz (blue) and $\beta_{\text{ref}} = 2.41$ and $f_{\text{m}} = 14.0$ GHz (solid red) produces a beat note at 3.6 GHz. These calculated amplitudes are scaled by redistributing a unity amplitude carrier among the sidebands, but probably don't represent the relative amplitudes of the interfering sidebands inside the detection apparatus. The main spectrum is truncated at the ±3rd–order sidebands and the vertical scale is linear.

In a phase modulated laser front-end comprised of single-mode polarization-maintaining (SMPM) fiber, and in some places polarizing PZ fiber, heterodyne detection of PM is an almost natural choice. Compared to heterodyne detection in free-space, where optical aberrations, beam tilts, imperfect beam overlap, polarization mismatch, refractive turbulence, higher-order spatial modes, and speckle, can all degrade performance, SMPM fiber and fiber-

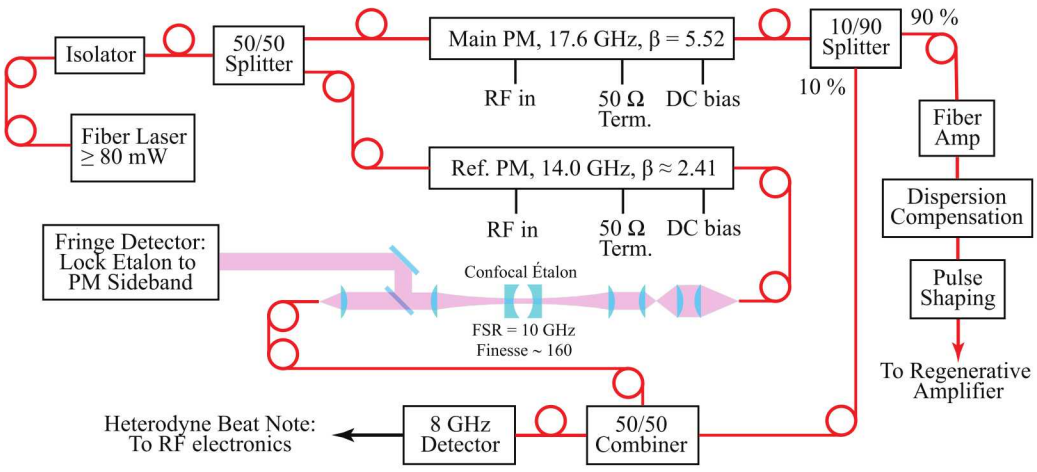

FIG. 2. Diagram of the laser and optical components that generate the heterodyne beat note and inject PM light into ZBL. The fiber laser's output (NP Photonics) is split 50/50, with one path entering the reference PM with $f_{\rm m}$ = 14.0 GHz, and the other entering the main PM with $f_{\rm m}$ = 17.6 GHz. A 10/90 splitter sends 90% of the light from the main PM to a fiber amplifier (IPG Photonics), followed by dispersion compensation and pulse shaping, and then into to the regenerative amplifier. The remaining 10% of the main PM light is sent to a 50/50 combiner. In the other path a confocal étalon selects and transmits a 1st–order sideband that is mixed with the 10% portion of the main PM light in the 50/50 combiner to generate the heterodyne signal. Approximately 10% of the reference sideband's light is sent to the fringe detector to stabilize the étalon. Long term lock to the first-order PM sideband is achieved by dithering the étalon's cavity length at 8 kHz to generate an error signal.

coupled components are ideal for obtaining a suitable beat note. The optical apparatus used in our PMFS is shown in Fig. 2.

Heterodyne detection is often associated with precision measurement techniques that may require a high degree of phase stability. Our use of heterodyne detection is much less demanding, so that single frequency fiber lasers provide more than adequate phase and amplitude stability. The only real consideration is whether the beat note is generated by splitting the amplitude of one laser, or uses two sufficiently stable lasers phase-locked to a reference with an appropriate offset frequency. Amplitude splitting forms a variation of a Mach-Zehnder interferometer, which at first glance might appear to require active relative-phase stabilization between its two paths, but we'll show in Sec. III B that this is unnecessary.

A. RF components for converting AM to the PMFS trigger signal

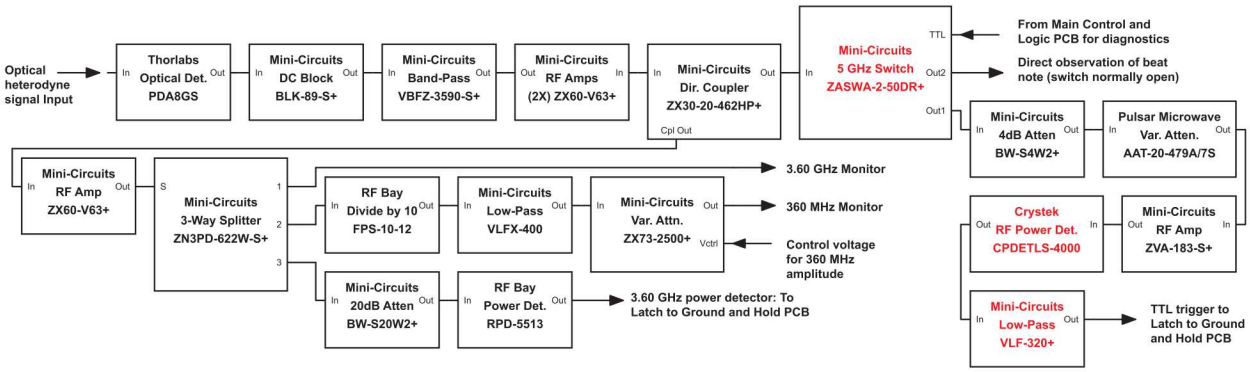

FIG. 3. RF components that generate the TTL level PMFS trigger signal. The 8 GHz optical detector (Thorlabs PDA8GS) generates $\leq$ 11.5 μW at 3.6 GHz, which rides on top of a DC pedestal. This signal is DC-blocked, bandpass filtered, pre-amplified, amplified, and followed by passive power conversion (Crystek CPDETLS-4000, 4 GHz bandwidth). Final filtering reduces the trigger's bandwidth to 0–320 MHz. The RF electronics also include high-speed switching for diagnostics (Mini-Circuits ZASWA-2-50DR+), variable attenuation to adjust the trigger level, and monitors at 3.6 GHz and 360 MHz. The $\div$10 (RF Bay FPS-10-12) has fixed output power, so the 3.6 GHz power is monitored to control the 360 MHz amplitude as the étalon in Fig. 2 is scanned across a 1st–order reference PM sideband. The RF components with red lettering are mentioned in the text .

Figure 3 shows the RF components that convert the 3.6 GHz electrical beat note into a TTL level DC signal whose falling edge is the trigger that indicates a PM failure. The process begins by removing a DC pedestal from the detector output followed by filtering, pre-amplification, attenuation for power control, final amplification, passive power detection, and a final low-pass filtering step. Using passive power detection this way doesn't require phase-sensitive electronic demodulation of AM at 17.6 GHz. Instead, optical heterodyne detection in effect demodulates by down-shifting the 17.6 GHz modulation frequency to the 3.6 GHz beat note that falls within the input bandwidth of the power detector.

A key component in this design is the passive RF power detector, a zero-bias Schottky diode with a bandwidth of 4 GHz. Although primarily intended for calibrated RF power measurements when terminated into high impedance, it also offers a simple solution for generating the failsafe trigger. To test it for high-speed applications we simulated PM

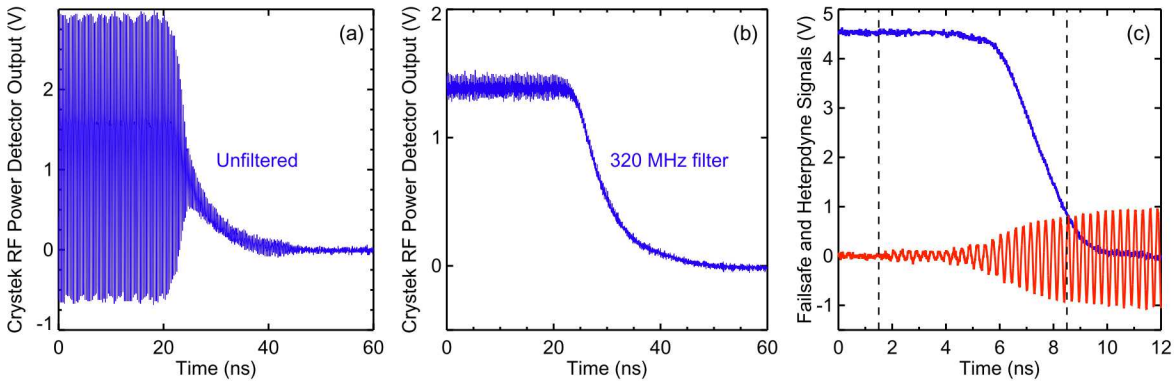

FIG. 4. Simulated failsafe events using the ZASWA-2-50DR+ switch in Fig. 3. (a) Unfiltered output of the RF power detector using an input frequency of 3.6 GHz and output termination of 50 Ω. The unfiltered signal is unsuitable for use as a failsafe trigger. (b) Same as (a) but after filtering with a bandpass of 0–320 MHz. The DC level of the trigger at the input to the high-speed OR gate in Fig. 5 would be higher for the same RF power because the input termination at the gate is 140 Ω, whereas termination on the oscilloscope is 50 Ω. (c) The failsafe signal for the same tests with the trigger adjusted to 3.5 V into 140 Ω. The optional 50 Ω output termination in Fig. 5 was used to ensure the failsafe remained below the 5 V limit of the oscilloscope. The heterodyne beat note shown in (c) comes from the normally open port on the ZASWA-2-50DR+ in Fig. 3 and indicates when the switch began to block the beat note for the normally closed port. If the trigger voltage is increased to 4 V the response time of the PMFS increases by 2–3 ns compared to about 7 ns shown here. These signals were recorded on a Tektronix DPO72004B oscilloscope with single-shot bandwidth of 18 GHz.

failures by switching off the amplified input at 3.6 GHz using the high-speed switch shown in Fig. 3 (Mini-Circuits ZASWA-2-50DR+). During these tests the simulated RF power at 3.6 GHz was similar to the power in the actual heterodyne beat note. When terminated into 1 MΩ, the DC-to-ground fall time exceeds 2 μs, which is too slow for a PMFS trigger. When terminated into 50 Ω its output consists of AM with $-0.7 \lesssim V_{\rm pp} \lesssim 3$ V, as shown in Fig. 4(a), so although the bandwidth is sufficiently high the signal is otherwise unusable. When followed by a 320 MHz low-pass filter, the output shown in Fig. 4(b) provides a useful trigger signal. There is residual AM, but its amplitude is sufficiently small relative to the trigger's DC level, and the fall time is about 10 ns. Ideally we want an even faster transition, and we also need a well defined threshold for a PM failure. These conditions are

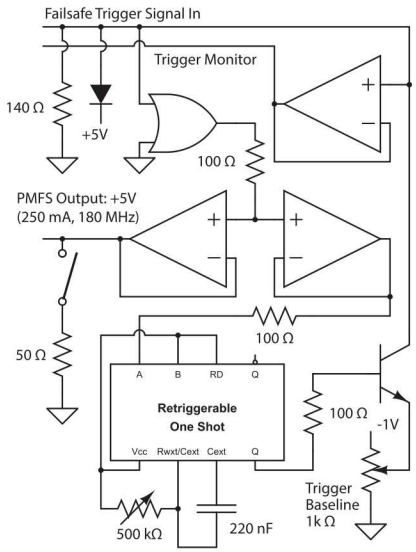

FIG. 5. Simplified diagram of the latch-to-ground-and-hold circuit. If a reduction in the heterodyne beat note amplitude pulls the trigger below the ~ 3.05 V transition threshold of the OR gate, its output goes low, and the one-shot drives the transistor base to pull the trigger close to ground for about 50 ms. During this time control circuitry shuts down the phase-locked oscillator (PLO) for 17.6 GHz so the PMFS can't restart or re-arm itself without operator intervention. The 50 Ω termination on the PMFS output is used for diagnostic purposes only.

met by setting the trigger level to just exceed the transition voltage of a high speed OR gate. Although this adds the OR gate's propagation delay of > 1 ns, the gate's fast falling edge results in a faster transition, as shown for the actual failsafe output in Fig. 4(c). Prior to any high–to–low transition, the PMFS must maintain approximately 5 V into 50 Ω, so the OR gate's output must be buffered, as shown in the simplified diagram of the PMFS' latch-to-ground-and-hold circuit in Fig. 5. The buffer's bandwidth is 180 MHz, which determines the final bandwidth for the failsafe output.

B. Stability of the optical heterodyne beat note and the PMFS trigger

The PM detection apparatus in Fig. 2 generates a heterodyne beat note with very good amplitude stability. This is achieved by optical filtering to select and transmit only the reference PM sideband, and by selecting β_{main} that has zero carrier amplitude, with two examples being $\beta = 5.52$ and $\beta = 8.654$. Although the system can operate reliably with

$\beta_{\rm main} \neq 5.52$, zero carrier amplitude also provides a useful visual cue to ZBL operators that the PMFS' main RF drive is functioning normally. In addition, $\beta = 5.52$ nearly coincides with a local maximum in the first-order sideband amplitude at $\beta \approx 5.33$. Although $\beta \approx 5.33$ maximizes the beat note amplitude, optimization is unnecessary as the sensitivity to small adjustments of $\beta_{\rm main}$ is low. For example, within the range $5.3 \lesssim \beta_{\rm main} \lesssim 5.7$, the beat note's $V_{\rm pp}$ changes by 6%, and the trigger's DC voltage changes by 3%.

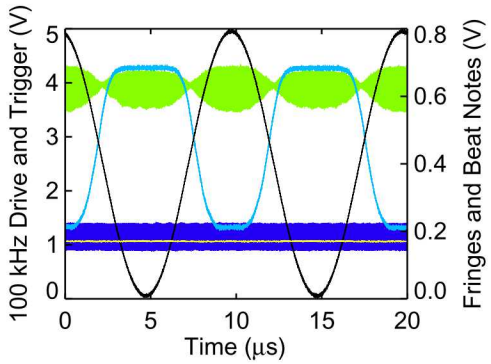

FIG. 6. Effects of a time varying phase shift of $\sim \pi$ radians on the behavior of the detection apparatus in Fig. 2, with and without the reference étalon installed. Black: The 0–5 V, 100 KHz sine wave attached to the high impedance DC bias port on the main PM, where $V_\pi \approx 5.6$ V. Light blue: Modulators off and reference étalon removed. Pure carrier interference results in fringes for a low finesse étalon. The detector saturates due to the higher than normal optical power. Green; heterodyne beat note with both PMs on, reference étalon removed, and $\beta_{\rm main}$ and $\beta_{\rm ref}$ near their nominal values but with a small amount of carrier interference. Dark blue: Normal operating conditions with $\beta_{\rm main} = 5.52$ and $\beta_{\rm ref} \approx 1.84$ and the étalon installed and locked to a 1st–order reference PM sideband. Yellow; The PMFS trigger signal resulting from the heterodyne beat note in dark blue. Waveforms were sampled at 10 ps per point to fully resolve the 3.6 GHz beat note. The trigger monitor is terminated into 50 Ω so the signal is below its nominal value of $\sim$ 3.5 V into 140 Ω. See text for a complete discussion.

During initial set up of the PMFS the reference PM spectrum is also set to have zero carrier amplitude, with $\beta_{\rm ref} = 2.41$. This is not a requirement for beat note stability, but merely a convenience, as $\beta_{\rm ref} = 2.41$ provides an easily identified starting point. After the reference étalon is locked to a 1st–order sideband, $\beta_{\rm ref}$ is subsequently set to ~ 1.84 to maximize the first-order sideband amplitude. This increases the electronic beat note power

from 10 μW (-20 dBm, $V_{\rm rms} \approx 22$ mV) to 11.5 μW (-19.4 dBm, $V_{\rm rms} \approx 24$ mV) at 3.6 GHz, which increases the trigger voltage by $\sim 9\%$.

Optimizing the beat note amplitude is simple, and demonstrating its stability is simple as well, however doing so requires making measurements for nonstandard operating conditions. As mentioned previously in Sec. III, the detection apparatus in Fig. 2 is effectively a Mach-Zehnder interferometer, which means the beat note stability could be susceptible to perturbations that induce a phase shift between its two paths. To demonstrate immunity to phase shifts we connected a 100 kHz sine wave source to the high-impedance DC bias port on the main modulator to induce a time varying relative phase of $\sim \pi$ radians. For the high impedance port $V_\pi \approx 5.6$ V. To check that varying the phase produces the expected behavior, we removed the confocal étalon from the reference path, turned off both phase modulators, and observed pure carrier interference. Figure 6 shows two cycles of the 0–5 V sine wave, along with fringes for a low finesse MZ interferometer. It also shows the beat note with the modulators on and with $\beta_{\rm main}$ and $\beta_{\rm ref}$ near their nominal values but with nonzero carriers, and the beat note amplitude is observed to fluctuate along with the phase shift. These signals were recorded directly from the 8 GHz optical detector, with no input to the RF components in Fig. 3, and without blocking the DC pedestal or using low-pass filtering. Although the PMFS trigger cannot be observed in this case, from Fig. 4(b) we know it would follow the beat note fluctuations. We also found that for any other operating condition that allows carrier interference, including with one modulator off, and with RF power for the other modulator adjusted to generate β with no observable carrier on a linear scale, we still observed étalon fringes that followed the applied phase shift, although the finesse was very low.

After resuming normal operation, with the étalon installed and detector output connected to the RF components in Fig. 3, the beat note and trigger were observed through their monitors, and as shown in Fig. 6, they are immune to the applied phase shift. These results demonstrate the necessity of using a moderately high finesse étalon to transmit only a single sideband to achieve reliable, stable operation for the amplitude splitting design in Fig. 2. The reference étalon has a measured finesse of ~ 160.

Although we're primarily concerned with amplitude stability, the beat note does display good long-term phase stability because the phase-locked oscillators (PLOs) that provide the PM drive are locked to the 10 MHz rubidium clock used to synchronize all timing signals for

ZBL. When sampled at 250 Hz, which is the rate for optical pulse formation, the beat note exhibits shot-to-shot phase jitter, but maintains long-term stability relative to the optical pulses. A high degree of phase stability isn't required because the trigger signal for the PMFS is derived from passive conversion of AM, and not from electronic demodulation.

C. Dependence of PM failsafe events on β for various trigger voltages

Because the heterodyne beat note is derived from the reference and main PM spectra, a change in either can initiate a failsafe event. Of real concern, of course, are changes in the main spectrum, and they can be characterized by setting the trigger's DC level at various values, followed by changes to the main RF power to vary β_{main}. For $\beta_{\text{main}} = 5.52$, the transition threshold for the OR gate in Fig. 5 occurs when a reduction in the heterodyne gain drops the trigger to about 3.05 V. Although the trigger's mean value is stable it contains enough residual AM, as shown in Fig. 4(b), that setting it ≤ 3.1 V could result in a spurious PM failure, so the trigger is normally set to about 3.5 V. Of interest, therefore, is the dependence of β_{main} at the onset of a failsafe event for trigger voltages of 3.1–3.5 V.

Figure 7(a) shows the measured main PM spectrum for $\beta = 5.52$ where the trigger threshold is ~ 3.05 V, and Figs. 7(b)–(d) show PM spectra at the onset of failsafe events for trigger voltages of 3.1 V, 3.3 V, and 3.5 V where the respective βs are 5.07, 4.83, and 4.71. These values correspond to reductions in β of approximately 8%, 13%, and 15%, where the changes in the main PM spectrum should not compromise safe operation of ZBL. Failsafe events also occur for increases in β because they also reduce the main PM first-order sideband amplitude, however given that scenario requires increased RF power it's probably a less likely failure mode, poses less risk, and therefore wasn't measured. The PM spectra in Fig. 7 were measured using a flat-flat scanning Fabry-Perot interferometer with an adjustable free spectral range set to ~ 320 GHz.

D. Suitability for detection of PM for nanosecond pulses

The PMFS for ZBL was designed for continuous monitoring of PM, however there's no fundamental reason it can't be used to detect PM on ns time scales, consistent with the ns pulses commonly used with multi-kJ laser systems. As discussed briefly in Sec. I, in

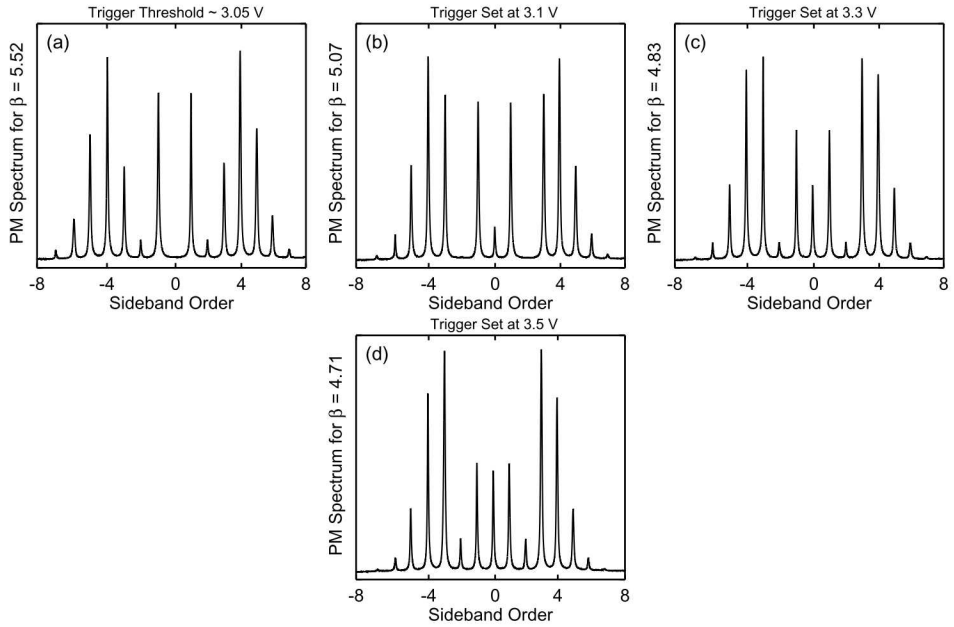

FIG. 7. Dependence of PM failsafe events on β for various trigger voltages. (a) For the nominal $\beta_{\text{main}} = 5.52$ the trigger threshold to initiate a PM failsafe event is about 3.05 V. (b)–(d) PM spectra at the onset of failsafe events for trigger voltages of 3.1 V, 3.3 V, and 3.5 V with respective βs of 5.07, 4.83, and 4.71. The vertical scale is linear and the relative amplitudes of the spectra are scaled against the tallest sidebands, which are $\pm$3rd–order for $\beta = 4.71$ in (d).

a laser front-end that generates multiple pre-pulses and a main pulse, where each may be modulated at a different PM frequency, PM is necessarily applied discretely in time. In such a system PM detection will likely occur within acquisition windows ≤ 5 ns. It's reasonable to ask if ZBL's heterodyne based PMFS could operate in this environment? For the circuit that monitors the trigger the answer is no because it accepts a continuous signal, but a sample-and-hold design could take its place. The question then remains, can heterodyne detection and passive AM power detection otherwise produce a usable trigger? Preliminary measurements suggest yes, however more RF gain might be necessary, and for pulse lengths ≤ 2 ns, a higher heterodyne beat note frequency might be required to obtain sufficient shot-to-shot stability. The examples of pulsed trigger signals in Fig. 8 suggest that for 3.6 GHz and pulses ≥ 4 ns, the stability would be sufficient to achieve performance comparable to what's achieved using continuous monitoring.

To test pulsed acquisition we replaced the 10% branch of the continuous, main PM signal that enters the 50/50 fiber combiner, as shown in Fig. 2, with phase modulated

pulses directly from the pulse shaping apparatus. Normally the 90% branch of this signal is amplified prior to pulse shaping, however for these measurements the additional power was unnecessary, so the 90% branch was routed directly through the shaper, then into the 50/50 combiner. With the AWG set to generate square pulses of 1–6 ns, and with ≥ 7 mW CW optical power in the 90% branch sent to the shaper, the resulting minimum pulse energy was $\sim$ 2 nJ. After mixing with the reference wave in the 50/50 combiner, these pulses produced a trigger that might be used with redesigned electronics. However as shown in Fig. 8(a), fluctuations of approximately 50% of the trigger's V_{pp} for a 1 ns pulse were too large for the reproducibility we require. However when the pulse length is increased to 4 ns the fluctuations decrease dramatically, which suggests that a higher heterodyne beat note frequency might allow monitoring of shorter pulses. Unfortunately, there is no simple way to increase the heterodyne frequency in this system just for the purpose of these tests, because it would require replacing the PLOs and some other components. Nonetheless, increasing the heterodyne frequency is conceptually simple, and given zero-bias Schottky detectors are available at higher frequencies, the same passive AM detection scheme should remain viable.

IV. FAILSAFE OPERATION, BUILT-IN DIAGNOSTICS, AND MEASUREMENTS OF THE MARGIN OF SAFETY

The PMFS employs two methods of interrupting a full energy shot. Because it's crucial to periodically confirm the PMFS is operating as expected, it also contains built-in tests that allow ZBL operators to quickly check its performance. It also contains three fault monitors that can warn users of issues that don't necessarily prevent normal operation, but could lead to future problems. And finally, it allows users to externally trigger a PM failure event, a feature that is used for measuring the margin of safety. These subjects are discussed below.

A. Failsafe operation

There are two methods of preventing a full energy shot in the event of a PM failure. The first and most important is the high-to-low transition of the failsafe outputs, which are used to inhibit triggers for digital delay generators. A second, and mostly redundant method is to use a high-speed switch to block the triggers themselves, however as we'll explain in

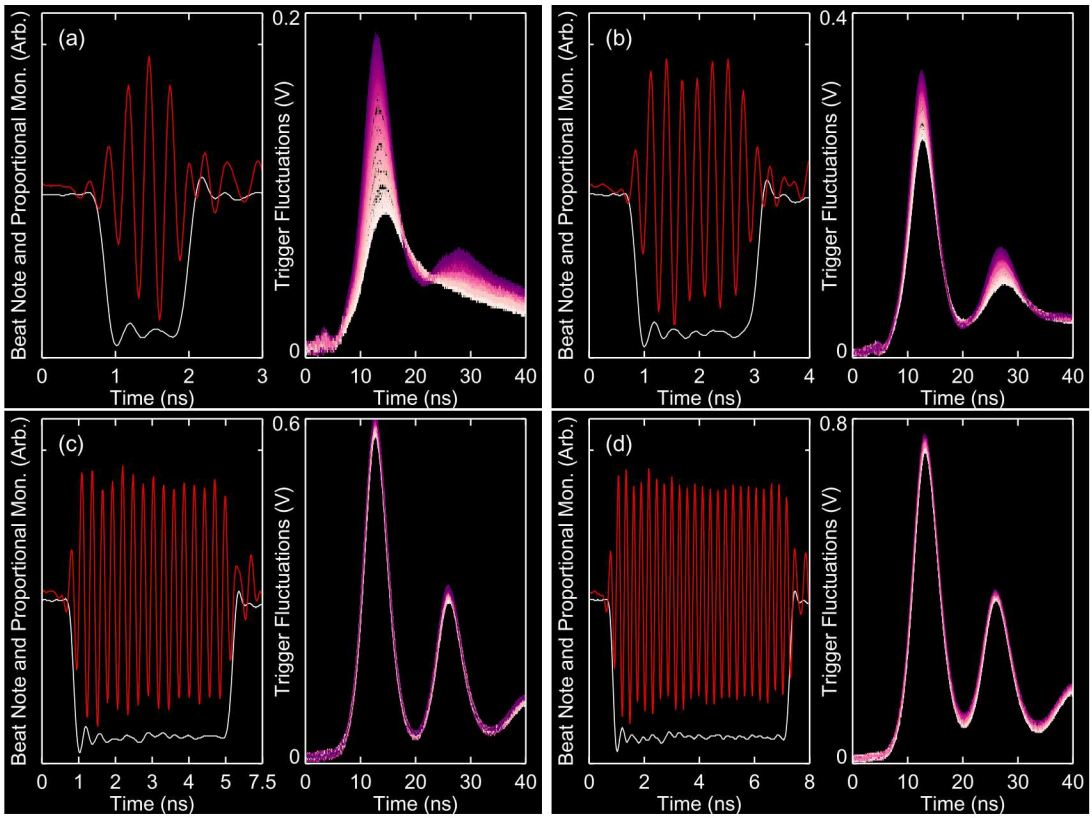

FIG. 8. Pulsed heterodyne detection of PM. (a) Left: A single-shot acquisition of the 3.6 GHz beat note and a 1 ns pulse from the AWG's proportional monitor; Right: Fluctuations in the trigger signal observed with the trigger monitor in Fig. 5 terminated into 50 Ω. A total of 205 shots were recorded at a rate of 250 Hz. The oscilloscope bandwidth was 5 GHz for all data at 20 ps/point with a 5k record length. (b) Same as (a) for a 2 ns pulse. (c) Four ns. (d) Six ns. The secondary peak in the trigger is probably ringing from an impedance mismatch, most likely due to the 140 Ω resistor at the input to the OR gate in Fig. 5. Ideally this resistor would be 50 Ω, however for continuous monitoring it was increased to 140 Ω to raise the trigger voltage to avoid operating one of the RF amps in Fig. 3 near saturation.

Sec. IV G, this approach doesn't necessarily offer a margin of safety for an instantaneous PM failure during initiation of a laser shot.

B. Single-shot PM failure test

The single-shot PM failure test allows operators to check that trigger inhibits controlled by the failsafe signal, or a trigger signal blocked by the PMFS, are operating as expected.

It does this by temporarily entering a failed state by blocking the heterodyne beat note using the ZASWA-2-50DR+ switch in Fig. 3. Functionality for this test, as well as the other diagnostic tests, is provided by a main control and logic circuit board. For a single-shot failure, the failsafe signal stays low for a little more than three "heartbeats," a 0.2 Hz clock signal that initiates the firing sequence for ZBL. After 3+ heartbeats the PMFS returns to normal operation without needing to be rearmed.

C. Gain and speed test

The gain and speed test repeatedly blocks the heterodyne beat note at a rate of 25 Hz, but without entering a failed state. This is used for setting the heterodyne gain so the trigger voltage is at the appropriate value, and also for checking the temporal response of the system. Monitors are provided for the trigger, the OR gate output and the one-shot Q pulse that drives the transistor base, as shown in Fig. 5. In addition, a 25 Hz square wave output serves as an oscilloscope trigger and timing fiducial. These same monitors, including an extra failsafe output, are always connected to an oscilloscope set for single event acquisition to display an actual PM failure, should one occur.

D. Failsafe current monitoring

Failsafe current monitoring detects two fault conditions that would most likely originate external to the PMFS, namely current that is too high or too low. The failsafe outputs were designed to maintain 5 V into 50 Ω indefinitely. They can also maintain 5 V into 25 Ω, which could occur with two 50 Ω trigger inhibit inputs driven in parallel, or if a user closed the switch for the 50 Ω output resistor in Fig. 5 while the failsafe is also terminated into 50 Ω. Whatever the cause of the high current, it's not considered a long-term safe operating condition. Low or no current would indicate termination into high impedance, which causes oscillation on the failsafe signal shown in Fig. 4(c), or it could also indicate a broken or damaged cable between the failsafe output and a trigger inhibit input on a delay generator. For either condition, front panel LEDs located at the failsafe outputs begin to blink, and an audible alarm sounds to warn operators about the abnormal failsafe current.

E. Fiber amplifier interlock status monitor

The fiber amplifier's interlock can be activated only when the PMFS is armed. The state of the interlock is available to ZBL operators through a high-speed buffer that monitors a logic gate that activates the interlock, and that signal can be monitored on an oscilloscope using single event triggering. If for any reason the interlock circuit becomes unstable, including coupling from external EM disturbances, the monitor can reveal glitches as short as 1 μs that may or may not trip the fiber amp. Inadvertent disabling of the fiber amp could result in a lost shot on ZBL. If the interlock is actually tripped and disables the fiber amp, an audible alarm sounds to alert ZBL operators.

F. Reference étalon dropout monitor

Under normal operating conditions the reference étalon in Fig. 2 will stay locked indefinitely. Nonetheless, stable long-term lock depends on a lock-in amp used to demodulate the error signal (Stanford Research Systems SR510), and a servo amp (New Focus LB1005), and numerous external connections. If for any reason the étalon lock experiences a short-term dropout, ZBL operators need to be alerted so that any potential problem can be diagnosed. The PMFS includes circuitry that monitors the reference étalon fringe signal, and if that signal falls below a threshold set by ZBL operators, a front panel status LED changes from green to red. The étalon dropout monitor is not intended to catch high speed glitches, and will respond only after the fringe signal falls below threshold for approximately 130 μs.

G. Externally triggered PM failure: Measuring the margin of safety

The margin of safety is the most important performance parameter for the PMFS because it ensures a full energy shot can be avoided no matter when a PM failure occurs. We define it as the time between two events: (1) The departure of a light pulse from the shaper, which along with the PMFS is housed in a master oscillator room (MOR), and (2) the latest time post-departure that a PM failure can occur that prevents that same pulse from passing through a Pockels cell known as the slicer. The slicer is triggered to transmit the pulse as it exits the regenerative amplifier and enters ZBL's main amplification chain. The margin of safety exists if event (2) occurs after event (1), which is not necessarily

guaranteed, but required for the PMFS to offer true engineered safety in the event of a perfectly timed and almost instantaneous PM failure. The existence of the margin of safety also means an otherwise good shot can be canceled at the very last moment. Because ZBL supports experiments on Sandia's Z Accelerator,[22] with x-ray radiography and ICF target preheating being two examples, the margin of safety could compromise experimental results, but eliminating the possibility of severe damage to ZBL has higher priority. Although measuring the margin of safety requires knowing propagation delays within the PMFS, and also for certain external signals, the test itself is otherwise simple.

When an optical pulse leaves the shaper it enters a 30 m long PZ fiber that delivers it to the regenerative amplifier. After a preset number of trips around the regen, it's coupled out and passes through the slicer Pockels cell. At this point a sampling optic can couple a small fraction of the regen's output into a fiber that returns it to the MOR. The return time for the regen pulse doesn't matter, but it does indicate if the slicer was disabled in time to stop the pulse from entering the main amplifiers. Timing of the PM failure for this test, relative to the heartbeat, is controlled by our final diagnostic tool, the externally triggered failure input.

For the 30 m length of the PZ fiber out to the regen, and for the current number of regen round trips, interrupting the heterodyne beat note using the ZASWA-2-50DR+ in Fig. 3 by means of the externally triggered failure input, reveals a margin of safety of ~ 50 ns. This result is representative of a failure in the RF electronics in Fig. 3, however there are other possible modes of failure, such as the phase modulators themselves. To test this other case, we can also induce a PM failure using the DC bias port for the 14.0 GHz reference phase modulator in fig. 2. The DC port can be accessed through a front panel connector, and by driving a pulse from a digital delay generator into this port, the heterodyne beat note amplitude is momentarily reduced by perturbing the phase of the reference PM spectrum. The bandwidth of the servo loop involved in locking the reference étalon in Fig. 2 is intentionally very low, so the servo ignores this disruption and the étalon remains locked, but the PMFS responds immediately. Using this method to initiate a PM failure results in a margin of safety of ~ 30 ns. Both measured values for the margin of safety could be increased by increasing the length of the PZ fiber, however there is no compelling reason to do so. The pre-pulse/main-pulse format generated by the shaper can change the measured margin of safety by ≤ 4 ns, however repeated measurements of the margin of safety using

the same pulse format were reproducible with resolution ≤ 1 ns.

Finally, in Sec. IV A we mentioned that blocking a trigger instead of activating the trigger inhibit on a delay generator, doesn't necessarily offer a margin of safety, and the reason for this is simple. For almost all easily accessible triggers that can be routed through the PMFS' trigger blocking switch, the propagation delays don't add up favorably, as they do when inhibiting the trigger for the slicer Pockels cell. The 30 m long fiber out to the regen, combined with the time a pulse circulates inside the regen, provide sufficient delay to obtain a suitable margin of safety.

V. CONCLUSIONS

We have developed and deployed a high speed phase modulation failsafe system for multi-kJ lasers based on continuous monitoring of an optical heterodyne signal, followed by passive AM power detection. The PMFS can respond to a PM failure in as little as 7 ns. In the Z-Beamlet facility at Sandia National Laboratories, this response time provides a margin of safety against accidental injection of single frequency light that ranges from 30–50 ns, depending on the origin of the PM failure. This technique offers very good long-term stability, good sensitivity to changes in the PM spectrum, and effectively hands-off operation to conform with engineered safety. The PMFS will maintain an armed condition effectively indefinitely, or until it's intentionally tripped by a human operator. Although the electronics in this PMFS were designed for continuous monitoring, so that a failure can be detected without using any timing signals, we've shown that heterodyne detection combined with passive AM detection could also be employed with redesigned electronics to detect PM for ns time scale pulses.

ACKNOWLEDGMENTS

Sandia National Laboratories is a multimission laboratory managed and operated by National Technology & Engineering Solutions of Sandia, LLC, a wholly owned subsidiary of Honeywell International Inc., for the U.S. Department of Energys National Nuclear Security Administration. With main facilities in Albuquerque, N.M., and Livermore, C.A., Sandia has major R&D responsibilities in national security, energy and environmental technologies,

and economic competitiveness.

This paper describes objective technical results and analysis. Any subjective views or opinions that might be expressed in the paper do not necessarily represent the views of the U.S. Department of Energy or the United States Government

REFERENCES

[1]R. Y. Chiao, C. H. Townes, and B. P. Stoicheff, Phys. Rev. **170**, 358 (1968).

[2]J. L. Emmett and A. L. Schawlow, Phys. Rev. **170**, 358 (1968).

[3]D. Heiman, D. S. Hamilton, and R. W. Hellwarth, Phys. Rev. B **19**, 6538 (1979).

[4]J. R. Smith, J. R. Murray, D. T. Kyrazis, R. B. Wilcox, T. L. Weiland, R. B. Ehrlich, C. E. Thompson, R. B. Engle, and A. E. Brown, Proc. SPIE **1047**, 219 (1989).

[5]J. R. Murray, J. R. Smith, R. B. Ehrlich, D. T. Kyrazis, C. E. Thompson, T. L. Weiland, and R. B. Wilcox, J. Opt. Soc. Am. B **6**, 2402 (1989).

[6]J. M. Eggleston and M. J. Kushner, Opt. Lett. **12**, 410 (1987).

[7]J. H. Campbell, P. A. Hurst, D. D. Heggins, W. A. Steele, and S. E. Bumpas, Proc. SPIE **2966**, 106 (1996).

[8]M. Bowers, S. Burkhart, S. Cohen, G. Erbert, J. Heebner, M. Hermann, and D. Jedlovec, Proc. SPIE **6451**, 64511M (2007).

[9]J.-F. Gleyze, J. Hares, S. Vidal, N. Beck, J. Dubertrand, and A. Perrina, Proc. SPIE **7916**, 79160I (2011).

[10]C. Dorrer, R. Roides, R. Cuffney, A. V. Okishev, G. B. W. A. B., A. Consentino, E. Hill, and J. D. Zuegel, IEEE J. Sel. Tp. Quantum Electron. **19**, 3500112 (2013).

[11]S. Hocquet, D. Penninckx, J.-F. Gleyze, C. Gouédard, and Y. Jaouën, Appl. Opt. **49**, 1104 (2010).

[12]S. Skupsky, R. W. Short, T. Kessler, R. S. Craxton, S. Letzring, and J. M. Soures, J. Appl. Phys. **66**, 3456 (1989).

[13]J. E. Rothenberg, J. Opt. Soc. Am. B **14**, 1664 (1997).

[14]J. E. Rothenberg, D. F. Browning, and R. B. Wilcox, Proc. SPIE **3492**, 51 (1999).

[15]S. Hocquet, D. Penninckx, E. Bordenave, C. Gouédard, and Y. Jaouën, Appl. Opt. **47**, 3338 (2008).

[16]S. Vidal, J. Luce, and D. Penninckx, Opt. Lett. **36**, 88 (2011).

[17]H. Cao, X. Lu, L. Li, X. Yin, W. Ma, J. Zhu, and D. Fan, Appl. Opt. **50**, 3609 (2011).

[18]D. Xu, Z. Huang, J. Wang, M. Li, H. Lin, R. Zhang, N. Zhu, Y. Zhang, and X. Tian, J. Opt. **15**, 1 (2013).

[19]P. Rambo, J. Schwarz, M. Schollmeier, M. Geissel, I. Smith, M. Kimmel, C. Speas, J. Shores, D. Armstrong, J. Bellum, E. Field, D. Kletecka, and J. Porter, Proc. SPIE **10014**, 100140Z (2016).

[20]M. R. Gomez, S. A. Slutz, A. B. Sefkow, D. B. Sinars, K. D. Hahn, S. B. Hansen, E. C. Harding, P. F. Knapp, P. F. Schmit, C. A. Jennings, T. J. Awe, M. Geissel, D. C. Rovang, G. A. Chandler, G. Cooper, M. E. Cuneo, A. J. Harvey-Thompson, M. C. Herrmann, M. H. Hess, O. Johns, D. C. Lamppa, M. R. Martin, R. D. McBride, K. J. Peterson, J. L. Porter, G. K. Robertson, G. A. Rochau, C. L. Ruiz, M. E. Savage, I. C. Smith, W. A. Stygar, and R. A. Vesey, Phys. Rev. Lett. **113**, 155003 (2014).

[21]M. Geissel, A. J. Harvey-Thompson, T. J. Awe, D. E. Bliss, M. E. Glinsky, M. R. Gomez, E. Harding, S. B. Hansen, C. Jennings, M. W. Kimmel, P. Knapp, S. M. Lewis, K. Peterson, M. Schollmeier, J. Schwarz, J. E. Shores, S. A. Slutz, D. B. S. nd I. C. Smith, C. S. Speas, R. A. Vesey, M. R. Weis, and J. L. Porter, Phys. Plasmas **25**, 022706 (2018).

[22]http://www.sandia.gov/z-machine/.